How to cite: *Angew. Chem. Int. Ed.* **2022,** *61,* e202115472
International Edition: doi.org/10.1002/anie.202115472
German Edition: doi.org/10.1002/ange.202115472

Photodecaging

Ligand-Directed Caging Enables the Control of Endogenous DNA Alkyltransferase Activity with Light inside Live Cells

*Yixin Zhang[+], Lili Han[+], Xiaoxu Tian, Chao Peng, and Yiyun Chen**

Abstract: The control of endogenous protein activity with light inside live cells is helpful for the high spatiotemporal probing of their dynamic roles. Herein, we report the first small-molecule-ligand-directed caging approach to control the endogenous human O^6-alkylguanine-DNA alkyltransferase (AGT) activity with light, and the caged AGT is constructed from the native intracellular AGT. The photo-responsive O^6-benzylguanine derivative O^6-NBG3 is developed to site-specifically cage the AGT's catalytic cysteine residue, and the light irradiation on-demand restores AGT's activity in vitro, in bacteria, and in mammalian cells. With O^6-NBG3, the alkylated AGT is dealkylated for the first time to recover the DNA repair activity in breast cancer MCF-7 cells by the dose-dependent light irradiation. This decaging strategy enables the localized modulation of endogenous AGT activity with high temporal precision without genetic engineering, which holds great potential for therapeutic applications.

Introduction

The control of proteins activity with light helps their biological roles probing in high spatiotemporal precision.[1] The optogenetic modulation methods in neuroscience and related life science researches utilize photosensitive proteins, which are incorporated by genetic engineering.[2] Among the optogenetic methods, the photocaged protein strategy is unique to modulate protein functions by the site-specific photodecaging of protein active sites (Figure 1).[3] Previously, the caged proteins were constructed by the genetic incorporation of unnatural amino acids (UAA) (Figure 1a). In the UAA incorporation method, rounds of directed evolution generated the UAA-specific aminoacyl-tRNA mutate synthetase and the mutate tRNA as the orthogonal pair, which genetically encoded the amber codon TAG to the caged UAA.[4] While effective, the technical barriers of

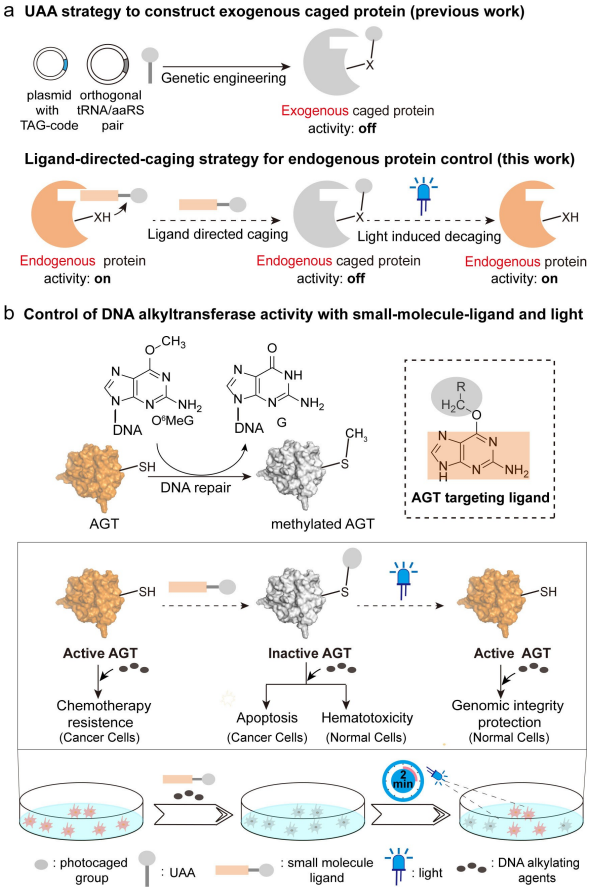

Figure 1. Methods for protein activity control with light and their applications on AGT modulation. a) Caged protein construction by the orthogonal UAA genetic incorporation for exogenous proteins (previous work), or by the small-molecule-ligand-directed caging for endogenous proteins (this work). b) The biological roles of AGT (O^6-alkylguanine-DNA alkyltransferase) and its localized control with light in high temporal precisions.

[*] Y. Zhang,[+] L. Han,[+] Y. Chen
State Key Laboratory of Bioorganic and Natural Products Chemistry, Centre of Excellence in Molecular Synthesis, Shanghai Institute of Organic Chemistry, University of Chinese Academy of Sciences, Chinese Academy of Sciences,
345 Lingling Road, Shanghai 200032 (China)
E-mail: yiyunchen@sioc.ac.cn

L. Han,[+] Y. Chen
School of Physical Science and Technology, ShanghaiTech University,
100 Haike Road, Shanghai 201210 (China)

Y. Chen
School of Chemistry and Material Sciences, Hangzhou Institute for Advanced Study, University of Chinese Academy of Sciences,
1 Sub-lane Xiangshan, Hangzhou 310024 (China)

X. Tian, C. Peng
National Facility for Protein Science in Shanghai, Zhangjiang Lab, Shanghai Advanced Research Institute, Chinese Academy of Science, Shanghai 201210 (China)

[+] These authors contributed equally to this work.

© 2022 Wiley-VCH GmbH

the orthogonal UAA incorporation method exist.[5] More importantly, the genetic engineering is not suitable for the endogenous protein modulation, which is required for studying native protein functions with further therapeutic applications.[6]

To this end, the small-molecule approach provides an attractive alternative. The photo-release of small molecules was previously developed for the endogenous protein activity control with light, however the unlimited free diffusion of released small molecules compromised the spatiotemporal precision of this method.[7] Scientists once reported the caged carbonic anhydrase I (CAI) construction from the CAI inhibitor tethering an acyl imidazole moiety, and the caged CAI could be decaged in vitro by the light irradiation.[8] However, the high reactivity of the acyl imidazole resulted in the random modification of non-catalytic protein residues, which was unsuitable for live-cell applications. We hypothesize that the careful choice of small-molecule-ligands and caging groups may enable the site-specific construction of caged proteins in live cells.

The O^6-guanine methylation in DNA induces the O^6MeG-T mismatch instead of the correct G–C pair, which results in transcriptional stalling, lesion bypass, and mutagenesis.[9] O^6-Alkylguanine-DNA alkyltransferase (AGT) selectively recognizes O^6MeG and transfers the methyl group to its cysteine-145 residue for the DNA repair (Figure 1b).[10] In normal cells, the AGT correction of O^6MeG protects the genomic integrity. In cancer cells, however, AGT defends the tumors by consuming the chemotherapeutic alkylating agents.[11] Various AGT covalent inhibitors have been developed to improve the chemotherapy efficacy by inducing the apoptosis.[12] However, the global AGT inhibition increases the normal cell mutation risks and results in hematotoxicity as the systemic side effect.[13] We envision that the localized AGT modulation with temporal precision may enable the AGT function rescue in normal cells for the genomic integrity protection, while the selective AGT inhibition in cancer cells induces the desirable apoptosis. The on-demand AGT modulation method may also probe AGT's heterogeneous expression in tumors and discover its new non-repair roles.[14] Herein, we present the first small-molecule-ligand-directed caging method to control AGT activity with light, which imposes significant challenges to current technologies due to the facile degradation of the alkylated AGT in live mammalian cells.[15]

Results and Discussion

We started with alkylguanine derivatives to test their AGT inhibition, hypothesizing the effective molarity from the AGT-alkylguanine interactions may improve the alkyl transfer selectivity (Figure 2a).[12a,16] Based on the structure of O^6-benzylguanine (O^6-BG), we designed and synthesized O^6-NBG1 as the light-responsive derivative. To evaluate its caging efficiency for AGT (20 μM), we incubated O^6-NBG1 (400 μM) in pH 7.4 Tris-HCl buffer at 37 °C for 2 hours. After the small molecule fraction removal by the size-exclusion column, the AGT's alkyl transfer reactivity indicator, O^6-BGFL, was added to measure the remaining alkyl transfer reactivity of AGT (see Figure S1 for assay details).[17] Pleasingly, we observed 70 % inhibition of the AGT's alkyl transfer reactivity from the O^6-NBG1 treatment (Figure 2b), and the *ortho*-substitutions in O^6-BG was tolerated.[18] LC-MS/MS analysis further confirmed that the *ortho*-nitrobenzyl group selectively modified the Cys145 residue of AGT (GNPVPILIPC145HR), while other spatially neighboring nucleophilic residues Tyr158, His146, or Ser159 were not modified (Figure S2).

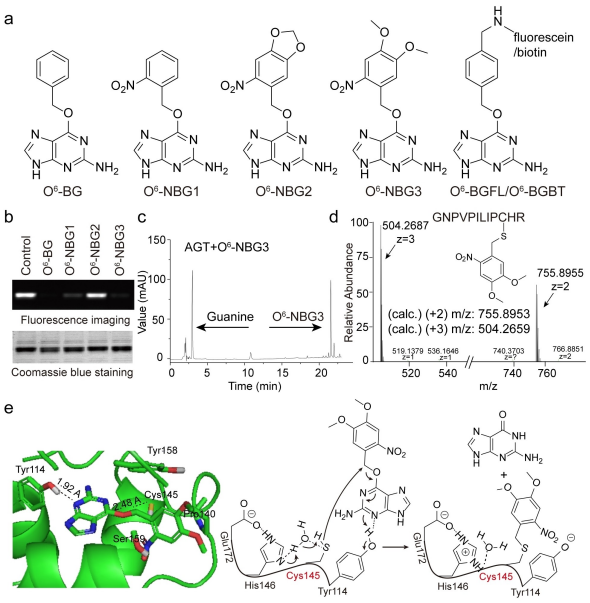

Figure 2. Design, synthesis, and evaluation of the AGT-targeting small-molecule-ligands for the AGT caging. a) The structures of AGT-targeting small-molecule-ligands. b) In-gel fluorescence analysis with O^6-BGFL on the AGT activity after the small-molecule-ligands treatment. c) HPLC analysis of the guanine formation after the O^6-NBG3 incubation with AGT. d) LC-MS/MS characterization of the O^6-NBG3-caged AGT. e) The docking analysis and mechanistic proposal of the O^6-NBG3 reaction with AGT.

To further improve the AGT inhibition and enable the visible-light-decaging, we synthesized O^6-NBG2 bearing the methylenedioxyl group and O^6-NBG3 with the dimethoxyl groups (Figure S3).[19] O^6-NBG2 resulted in no AGT inhibition with >95 % remaining AGT activity, while O^6-NBG3 completely inhibited AGT activity together with the quantitative guanine formation (Figure 2b,c). The control experiment suggested that the O^6-NBG3 incubation in the absence of AGT gave no guanine formation (Figure S4). LC-MS/MS analysis confirmed that Cys145 in AGT was site-specifically modified by the 6-nitroveratryl group (Figure 2d, see Figure S5 for MS details). The ratio of the Cys145-modified peptide by O^6-NBG3 was higher than those from O^6-NBG1, consistent with the more effective O^6-NBG3 caging by the in-gel fluorescence analysis (Figure S2, S5). The proposed O^6-NBG3 caging mechanism is similar to the reported AGT's alkyl transfer mechanism (Figure 2e).[20] The water molecule first activates His146 for the Cys145 deprotona-

© 2022 Wiley-VCH GmbH

tion, and the deprotonated Cys145 attacks the O^6-benzyl group with Tyr114 assistance to afford the thiol-benzylated adduct and the eliminated guanine. The docking analysis between AGT and O^6-NBG3 reveals the *ortho*-nitrobenzyl group stacks between Pro140 and Ser159, which explains the *ortho*-substitution tolerance on O^6-NBG3. The *meta*- and *para*- methoxy group substituents on O^6-NBG3 accelerate the reaction with the increased electro-negativity by the extra π–π stacking interaction with Try158.

We next tested if the light irradiation could recover the AGT activity caged by O^6-NBG3 (Figure 3). It is well known that the AGT alkylation triggers the conformational changes and leads to the AGT degradation after the facile ubiquitylation. It remains unclear if the dealkylation results in the AGT activity recovery.[15,21] Pleasingly, a handheld UV LED lamp irradiation (365 nm, 12 mW cm^{-2}) for 20 minutes recovered >60 % AGT activity from the O^6-NBG3-caged AGT (Figure 3a, Figure S6). The photodecaging reaction was significantly accelerated by the higher intensity irradiation, and the use of a UV LED dot light (365 nm, 650 mW cm^{-2}) for merely 30 seconds recovered >60 % AGT activity (Figure 3b). Light irradiation with a longer wavelength may improve biocompatibility and increase better cell penetration.[22] We found that the violet LED dot light (405 nm, 650 mW cm^{-2}) irradiation for 5 minutes recovered >70 % AGT activity.[23] LC-MS/MS analysis confirmed that the Cys145 residue was effectively recovered by the light irradiation, in contrast to the trace amount of free Cys145 detected before the light treatment (Figure 3c). This is the first dealkylation reported for the alkylated AGT and confirms the AGT dealkylation indeed recovers the AGT activity.[24]

The AGT activity control with O^6-NBG3 and light was further tested in the biological contexts (Figure 4a). In the pH 7.4 Tris buffer containing different reactive biomolecules

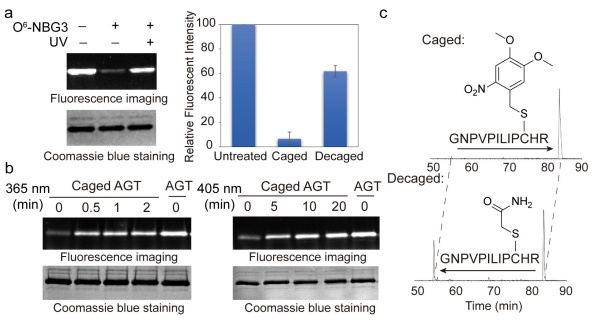

Figure 3. Photodecaging of the O^6-NBG3-caged AGT in vitro. a) O^6-NBG3-caged AGT activity after light irradiation in vitro with the O^6-BGFL in-gel fluorescence analysis. The O^6-NBG3-caged AGT was irradiated by a UV lamp (365 nm, 12 mW cm^{-2}) for 20 min. The error bars represent the standard deviation of triplicate experiments. b) Time-dependent O^6-NBG3-caged AGT activity after a UV LED dot light irradiation (365 nm, 650 mW cm^{-2}, left panel) or violet LED dot light irradiation (405 nm, 650 mW cm^{-2}, right panel) with the O^6-BGFL in-gel fluorescence analysis. c) LC-MS/MS characterization of the O^6-NBG3-caged AGT before and after the irradiation. The cysteine residues on caged or decaged AGT samples were alkylated by iodoacetamide before the MS characterization.

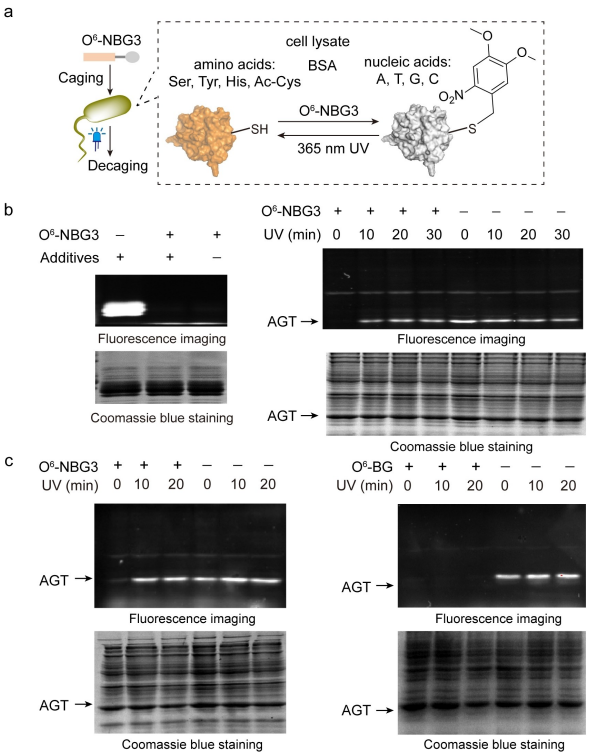

Figure 4. The AGT control with O^6-NBG3 and light in the biological contexts and in live bacterial cells. a) Schematic illustration for the O^6-NBG3 modulation in the biological contexts and in live bacteria cells. b) AGT caging with O^6-NBG3 (400 μM) in the presence of biologically relevant additives (left panel), and the decaging of the O^6-NBG3-caged AGT in cell lysates (right panel) with the O^6-BGFL fluorescence analysis. c) Photodecaging of the O^6-NBG3-caged AGT (left panel) or the O^6-BG-blocked AGT (right panel) in live bacterial cells with the O^6-BGFL fluorescence analysis. O^6-NBG3 and O^6-BG (400 μM) were incubated in the AGT-overexpressed *E. coli* for 3 hours, respectively, before the handheld UV LED light irradiation (365 nm, 12 mW cm^{-2}).

(amino acids serine, tyrosine, histidine, acetylcysteine, nucleic acids dNTPs, and proteins BSA in equal moles or masses) or *E. coli* cell lysates (2 mg mL^{-1}), the AGT inhibition by O^6-NBG3 (400 μM) was not affected.[25] In addition, the O^6-NBG3 incubation in the absence of AGT resulted in no O^6-NBG3 consumption by these biomolecules (Figure S7). The decaging reaction with a handheld UV LED lamp (365 nm, 12 mW cm^{-2}) for 10 min recovered >95 % AGT activity in *E. coli* cell lysates (2 mg mL^{-1}, Figure 4b). These results confirmed the effective modulation of AGT by O^6-NBG3 in complex biological contexts and suggested its live-cell applications.

We next conducted the intracellular O^6-NBG3 modulation in the AGT-overexpressed bacteria (Figure 4c). With O^6-NBG3 (400 μM) in the cell medium, the loss of intracellular AGT activity was observed after 1-hour O^6-NBG3 incubation. After an extended 4-hour incubation, very little residual AGT activity could be detected by the O^6-BGFL fluorescence analysis in the cell lysate (Figure S8). We removed the remaining O^6-NBG3 by the buffer exchange with the fresh cell medium, and irradiated the cells with a handheld UV LED light (365 nm, 12 mW cm^{-2}). The O^6-

© 2022 Wiley-VCH GmbH

NBG3-caged bacteria recovered >95 % AGT activity after 10-minute irradiation, while the cells treated by O^6-BG observed no AGT activity recovery after the extended light irradiation. These results together suggested its potential for live mammalian cell applications.

In mammalian cells, AGT exists both in the cytoplasm and nucleus. The cysteine-145 alkylated AGT undergoes facile degradation from various ubiquitination pathways.[15b,26] These complications posed daunting challenges for constructing the caged AGT by the UAA incorporation method, and no light-modulation approach of AGT has been reported. We hypothesize that the fast chemical caging efficiency of O^6-NBG3 may circumvent the facile AGT degradation and constructs the caged AGT (Figure 5a). In fact, the 3-hour O^6-NBG3 (300 μM) incubation inhibited >80 % AGT activity in the human embryonic kidney cells (HEK 293T) transfected with AGT (Figure 5b).[27] The O^6-NBG3-treated HEK 293T cells were next irradiated with a handheld UV LED light (365 nm, 12 mW cm^{-2}), and ≈50 % AGT activity recovery was observed after 3-minute irradiation. The extended 9-minute irradiation restored >75 % catalytic activity of AGT, demonstrating the dose-dependency of the light irradiation, and showcased the first AGT activity control with light in mammalian cells without genetic engineering.[28]

The endogenous AGT modulation is more relevant for its diagnostic and therapeutic applications; however, the low endogenous AGT level imposes technical challenges.[12c] To

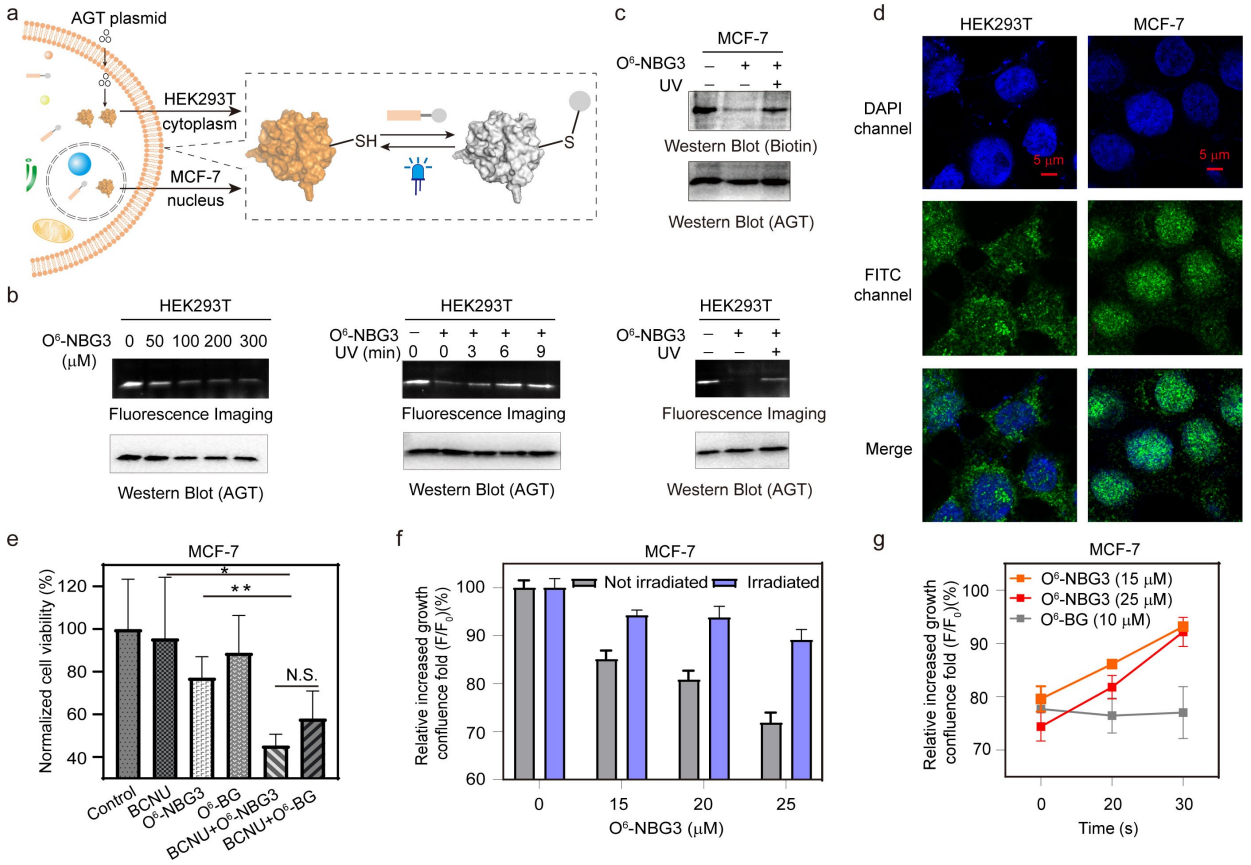

Figure 5. The AGT control with O^6-NBG3 and light inside mammalian cells, and the use as the photo-responsive chemotherapy adjuvants for MCF-7 cells. a) Schematic illustration of the AGT modulation inside live mammalian cells. b) The AGT modulation by O^6-NBG3 in HEK 293T cells, with the O^6-BGFL fluorescence analysis. O^6-NBG3 concentrations (left panel) and irradiation times (middle panel) were varied. The O^6-NBG3-caged AGT in HEK 293T was constructed by incubating with O^6-NBG3 (300 μM) for 3 hours in DMEM culture. The caged HEK 293T cells were irradiated with a hand-held UV lamp (365 nm, 12 mW cm^{-2}) for 3 minutes to restore the AGT activity (right panel). c) The endogenous AGT modulation by O^6-NBG3 and light in MCF-7 cells, with O^6-BGBT western blot analysis. The O^6-NBG3-caged AGT in MCF-7 cells was constructed by incubating with O^6-NBG3 (100 μM) for 3 hours in DMEM culture and decaged with the identical conditions as in HEK 293T cells. d) Confocal fluorescent imaging of the AGT location in AGT-overexpressed HEK293T or the MCF-7 cells. The anti-AGT antibody visualized the AGT after cell fixation. DAPI channel showed the nucleus location, and FITC channel showed the AGT distributions in mammalian cells. e) The MTT cell viability assay of MCF-7 cells against different small molecule (100 μM) treatments using the CCK-8 method, and error bars represented the standard deviation of triplicate experiments. P-value was calculated to evaluate the significant difference, $p<0.05$ (*), $p<0.01$ (**), $p>0.05$ (N.S.). Error bars represented mean ± SD ($n=3$). BCNU (Bis-chloroethylnitrosourea). f) The cells proliferation confluence analysis of MCF-7 cells upon BCNU (50 μM) treatment against different concentrations of O^6-NBG3 (0, 15, 20, 25 μM) and UV light (365 nm, 12 mW cm^{-2})irradiation for 20 seconds. g) The cells proliferation confluence analysis of MCF-7 cells upon BCNU (50 μM) treatment against the different duration (0, 20, 30 s) of light irradiation. The relative increased growth confluence fold was explored to eliminate the growth deviation resulting from the initial cell plating. F and F_0 mean the increased fold of cell growth confluence with and without O^6-NBG3 treatment. Error bars represented mean ± SD ($n=8$).

© 2022 Wiley-VCH GmbH

this end, we chose O^6-BGBT to analyze the endogenous AGT activity in breast cancer MCF-7 cells via the biotin-streptavidin western blot (Figure S9).[29] As a result, the incubation of O^6-NBG3 (100 μM) for 3 hours resulted in >80 % AGT activity inhibition in MCF-7 cells, and a handheld UV LED light (365 nm, 12 mW cm^{-2}) irradiation for 3 minutes recovered >75 % AGT activity (Figure 5c). We next used confocal fluorescent microscopy to visualize the overexpressed and endogenous AGT localization with the anti-AGT immunoimaging (Figure 5d). The overexpressed AGT in HEK 293T cells was observed mainly in the cytoplasm. In contrast, the endogenous AGT in MCF-7 cells was mainly in the nucleus. These results further suggested the unique advantages of this small-molecule-ligand-directed caging method to study endogenous proteins.[32] With this method, the alkylated endogenous AGT in breast cancer cells was dealkylated for the first time to restore its DNA repair activity, which may provide insights for the AGT′s heterogeneous expression probing in tumors and AGT′s novel physiological roles discovery.

Bis-chloroethylnitrosourea (BCNU) is a commonly used chemotherapy drug as the DNA alkylating reagent.[10] The exposure of BCNU (400 μM) to MCF-7 cells killed 70 % of cancer cells (30 % survival rate, Figure S10); however, the high concentrations of BCNU resulted in numerous undesirable side effects.[10] In contrast, 100 μM of BCNU had fewer side effects but only killed <5 % cancer cells (>95 % survival rate, Figure 5e BCNU). We then tested O^6-NBG3 (100 μM) as the chemotherapeutic adjuvants and found the O^6-NBG3/BCNU cocktail killed >60 % cancer cells with only 100 μM of BCNU (Figure 5e BCNU + O^6-NBG3). These adjuvant effects were similar to the O^6-BG/BCNU cocktail with ≈50 % cancer cell killing (Figure 5e BCNU + O^6-BG),[18a,30] which indicated O^6-NBG3 as the effective chemotherapeutic adjuvants to inactivate AGT in MCF-7 cells.

We further evaluated the combined use of O^6-NBG3 and light irradiation to modulate AGT activity in response to the BCNU treatment in mammalian cells (Figure 5f, g, Figure S11). The real-time cell imaging was recorded on the Incucyte live-cell imaging instrument to analyze the cell proliferation confluence. The O^6-NBG3 treatment resulted in decreased cell growth rates, which was consistent with the MTT cell viability assay in Figure 5e and indicated the O^6-NBG3 enhancement of cancer cells' BCNU sensitivity. The short light irradiation restored >90 % cell viability similar to blank cells (Figure 5f, Figure S11). The dose-dependency for the light irradiation was observed that the extended irradiation (365 nm, 12 mW cm^{-2}) further recovered the cell viability (Figure 5g). In contrast, the cells treated with O^6-BG showed no light response.[31] These results suggested O^6-NBG3 as the photo-responsive chemotherapeutic adjuvants for the endogenous AGT. The addition of O^6-NBG3 decreased the MCF-7 cells' tolerance to BCNU as shown in Figure 1b, while the localized irradiation reverted the AGT activity to recover the cell viability. This on-demand small-molecule-ligand modulation method has the potential to decrease the chemotherapeutic toxicity to normal cells with the on-demand light irradiation.

Conclusion

In conclusion, we have developed the first light-modulation method for controlling endogenous proteins activity inside live cells via the small-molecule-ligand-directed-caging strategy. The light-responsive O^6-alkylguanine derivatives selectively caged the catalytic cysteine residue of the DNA alkyltransferase, and the light irradiation on-demand activated AGT in minutes on the purified protein, inside live bacteria and mammalian cells. The small-molecule-ligand-directed-caging strategy is attractive to construct light-responsive proteins without genetic engineering, enabling site-specific turn-off and spatiotemporal turn-on of the endogenous proteins′ functions in live cells. The current photodecaging method provides the localized control of protein activity by the light irradiation, and we envision the photocatalytic decaging with the cell-type-selective photocatalysts may enable the cell-type-selective photodecaging,[1e,f,33] which are undergoing in our laboratory.

Acknowledgements

Financial support was provided by the National Natural Science Foundation of China 91753126, 21622207, 21602242, 21272260, CAS Interdisciplinary Innovation Team JCTD-2020-16, Program of Shanghai Academic/Technology Research Leader 21XD1424700, and Strategic Priority Research Program of the Chinese Academy of Sciences XDB20020200.

Conflict of Interest

The authors declare no conflict of interest.

Data Availability Statement

The data that support the findings of this study are available in the supplementary material of this article.

Keywords: DNA Alkyltransferases · Endogenous Protein Modulation · Photodecaging · Small-Molecule-Ligands

[1] a) N. Ankenbruck, T. Courtney, Y. Naro, A. Deiters, *Angew. Chem. Int. Ed.* **2018**, *57*, 2768–2798; *Angew. Chem.* **2018**, *130*, 2816–2848; b) B. R. Rost, F. Schneider-Warme, D. Schmitz, P. Hegemann, *Neuron* **2017**, *96*, 572–603; c) T. Fehrentz, M. Schoenberger, D. Trauner, *Angew. Chem. Int. Ed.* **2011**, *50*, 12156–12182; *Angew. Chem.* **2011**, *123*, 12362–12390; d) R. K. V. Lim, Q. Lin, *Acc. Chem. Res.* **2011**, *44*, 828–839; e) H. Wang, W.-G. Li, K. Zeng, Y.-J. Wu, Y. Zhang, T.-L. Xu, Y. Chen, *Angew. Chem. Int. Ed.* **2019**, *58*, 561–565; *Angew. Chem.* **2019**, *131*, 571–575; f) H. Wang, Y. Zhang, K. Zeng, J. Qiang, Y. Cao, Y. Li, Y. Fang, Y. Z. hang, Y. Chen, *JACS Au* **2021**, *1*, 1066–1075.

© 2022 Wiley-VCH GmbH

[2] a) E. S. Boyden, F. Zhang, E. Bamberg, G. Nagel, K. Deisseroth, *Nat. Neurosci.* **2005**, *8*, 1263–1268; b) K. Deisseroth, *Nat. Methods* **2011**, *8*, 26–29.

[3] a) T. Courtney, A. Deiters, *Curr. Opin. Chem. Biol.* **2018**, *46*, 99–107; b) N. Wu, A. Deiters, T. A. Cropp, D. King, P. G. Schultz, *J. Am. Chem. Soc.* **2004**, *126*, 14306–14307; c) A. Deiters, D. Groff, Y. H. Ryu, J. M. Xie, P. G. Schultz, *Angew. Chem. Int. Ed.* **2006**, *45*, 2728–2731; *Angew. Chem.* **2006**, *118*, 2794–2797.

[4] a) E. A. Lemke, D. Summerer, B. H. Geierstanger, S. M. Brittain, P. G. Schultz, *Nat. Chem. Biol.* **2007**, *3*, 769–772; b) J.-Y. Kang, D. Kawaguchi, I. Coin, Z. Xiang, D. D. M. O'Leary, P. A. Slesinger, L. Wang, *Neuron* **2013**, *80*, 358–370; c) D. P. Nguyen, M. Mahesh, S. J. Elsaesser, S. M. Hancock, C. Uttamapinant, J. W. Chin, *J. Am. Chem. Soc.* **2014**, *136*, 2240–2243.

[5] a) B. Yang, N. Wang, P. D. Schnier, F. Zheng, H. Zhu, N. F. Polizzi, A. Ittuveetil, V. Saikam, W. F. DeGrado, Q. Wang, P. G. Wang, L. Wang, *J. Am. Chem. Soc.* **2019**, *141*, 7698–7703; b) J. Wang, Y. Liu, Y. Liu, S. Zheng, X. Wang, J. Zhao, F. Yang, G. Zhang, C. Wang, P. R. Chen, *Nature* **2019**, *569*, 509–513; c) N. Elia, *FEBS J.* **2021**, *288*, 1107–1117.

[6] B. D. Allen, A. C. Singer, E. S. Boyden, *Learn. Mem.* **2015**, *22*, 232–238.

[7] a) M. W. H. Hoorens, W. Szymanski, *Trends Biochem. Sci.* **2018**, *43*, 567–575; b) W. A. Velema, W. Szymanski, B. L. Feringa, *J. Am. Chem. Soc.* **2014**, *136*, 2178–2191; c) J. M. Silva, E. Silva, R. L. Reis, *J. Controlled Release* **2019**, *298*, 154–176.

[8] K. Matsuo, Y. Kioi, R. Yasui, Y. Takaoka, T. Miki, S.-h. Fujishima, I. Hamachi, *Chem. Sci.* **2013**, *4*, 2573–2580.

[9] a) B. H. Hudson, H. S. Zaher, *RNA* **2015**, *21*, 1648–1659; b) L. Xu, W. Wang, J. B. Wu, J. H. Shin, P. C. Wang, I. C. Unarta, J. Chong, Y. S. Wang, D. Wang, *Proc. Natl. Acad. Sci. USA* **2017**, *114*, E7082–E7091; c) M. Ezerskyte, J. A. Paredes, S. Malvezzi, J. A. Burns, G. P. Margison, M. Olsson, D. A. Scicchitano, K. Dreij, *Proc. Natl. Acad. Sci. USA* **2018**, *115*, 4731–4736.

[10] S. L. Gerson, *Nat. Rev. Cancer* **2004**, *4*, 296–307.

[11] a) M. Christmann, B. Verbeek, W. P. Roos, B. Kaina, *BBA-Rev. Cancer* **2011**, *1816*, 179–190; b) A. E. Pegg, *Chem. Res. Toxicol.* **2011**, *24*, 618–639; c) C. A. Rabik, M. C. Njoku, M. E. Dolan, *Cancer Treat. Rev.* **2006**, *32*, 261–276.

[12] a) G. Sun, L. Zhao, R. Zhong, Y. Peng, *Future Med. Chem.* **2018**, *10*, 1971–1996; b) A. Sabharwal, M. R. Middleton, *Curr. Opin. Pharmacol.* **2006**, *6*, 355–363; c) C. Wang, D. Abegg, D. G. Hoch, A. Adibekian, *Angew. Chem. Int. Ed.* **2016**, *55*, 2911–2915; *Angew. Chem.* **2016**, *128*, 2964–2968.

[13] a) K.-H. Tomaszowski, N. Hellmann, V. Ponath, H. Takatsu, H.-W. Shin, B. Kaina, *Sci. Rep.* **2017**, *7*, 13925; b) B. Wängler, R. Schirrmacher, C. Wängler, *Tetrahedron Lett.* **2020**, *61*, 151840.

[14] a) A. C. Povey, C. N. Hall, D. P. Cooper, P. J. O'Connor, G. P. Margison, *Int. J. Cancer* **2000**, *85*, 68–72; b) M. Citron, R. Decker, S. Chen, S. Schneider, M. Graver, L. Kleynerman, L. B. Kahn, A. White, M. Schoenhaus, D. Yarosh, *Cancer Res.* **1991**, *51*, 4131–4134; c) A. G. M. Mostofa, S. R. Punganuru, H. R. Madala, K. S. Srivenugopal, *Neoplasia* **2018**, *20*, 305–323; d) A. Paranjpe, N. I. Bailey, S. Konduri, G. C. Bobustuc, F. Ali-Osman, M. A. Yusuf, S. R. Punganuru, H. R. Madala, D. Basak, A. Mostofa, K. S. Srivenugopal, *J. Biomed. Res.* **2016**, *30*, 393–410.

[15] a) M. Xu-Welliver, A. E. Pegg, *Carcinogenesis* **2002**, *23*, 823–830; b) B. Mollwitz, E. Brunk, S. Schmitt, F. Pojer, M. Bannwarth, M. Schiltz, U. Rothlisberger, K. Johnsson, *Biochemistry* **2012**, *51*, 986–994; c) E. Brunk, B. Mollwitz, U. Rothlisberger, *ChemBioChem* **2013**, *14*, 703–710.

[16] a) X. Y. Li, D. R. Liu, *Angew. Chem. Int. Ed.* **2004**, *43*, 4848–4870; *Angew. Chem.* **2004**, *116*, 4956–4979; b) V. M. Krishnamurthy, V. Semetey, P. J. Bracher, N. Shen, G. M. Whitesides, *J. Am. Chem. Soc.* **2007**, *129*, 1312–1320.

[17] a) A. Keppler, S. Gendreizig, T. Gronemeyer, H. Pick, H. Vogel, K. Johnsson, *Nat. Biotechnol.* **2003**, *21*, 86–89; b) C. Robinson, J. Palomo, M. A. Vogelbaum, *Anal. Biochem.* **2010**, *405*, 263–265.

[18] a) G. T. Pauly, N. A. Loktionova, Q. Fang, S. L. Vankayala, W. C. Guida, A. E. Pegg, *J. Med. Chem.* **2008**, *51*, 7144–7153; b) K. Mineura, M. Fukuchi, M. Kowada, I. Terashima, K. Kohda, *Int. J. Cancer* **1995**, *63*, 148–151.

[19] P. Klán, T. Šolomek, C. G. Bochet, A. Blanc, R. Givens, M. Rubina, V. Popik, A. Kostikov, J. Wirz, *Chem. Rev.* **2013**, *113*, 119–191.

[20] D. S. Daniels, C. D. Mol, A. S. Arvai, S. Kanugula, A. E. Pegg, J. A. Tainer, *EMBO J.* **2000**, *19*, 1719–1730.

[21] K. S. Srivenugopal, X. H. Yuan, H. S. Friedman, F. AliOsman, *Biochemistry* **1996**, *35*, 1328–1334.

[22] C. Hu, Y. Chen, *Tetrahedron Lett.* **2015**, *56*, 884–888.

[23] The compromised AGT activity recovery by light irradiation may be due to the conformational changes upon caging or the side reactions upon photodecaging, see Ref. [15c] and A. B. Smith, S. N. Savinov, U. V. Manjappara, I. M. Chaiken, *Org. Lett.* **2002**, *4*, 4041–4044.

[24] There has been no dealkylation pathway of the alkylated AGT discovered in live cells. The alkylated form of AGT was known to be ubiquitinated and degraded via the ubiquitin/proteasomal system. See Ref. [15].

[25] H. Huang, G. Zhang, L. Gong, S. Zhang, Y. Chen, *J. Am. Chem. Soc.* **2014**, *136*, 2280–2283.

[26] M. Belanich, T. Randall, M. A. Pastor, J. T. Kibitel, L. G. Alas, M. E. Dolan, S. C. Schold, M. Gander, F. J. Lejeune, B. F. L. Li, A. B. White, P. Wasserman, M. L. Citron, D. B. Yarosh, *Cancer Chemother. Pharmacol.* **1996**, *37*, 547–555.

[27] The residual AGT activity after O^6-NBG3 treatment may attribute to the poor water solubility and low uptake of O^6-NBG3 in mammalian cells. See Ref. [18].

[28] The decreased decaging efficiency in mammalian cells compared to bacteria was due to various possible degradation pathways from ubiquitination during the caging process. See Ref. [15].

[29] Due to the heterogeneous AGT expression in various cancer cell lines, the extremely low endogenous expression level of AGT was found in HEK293T cells and was not suitable for experimental investigations. See Refs. [10], [12c].

[30] M. E. Dolan, R. C. Moschel, A. E. Pegg, *Proc. Natl. Acad. Sci. USA* **1990**, *87*, 5368–5372.

[31] The UV irradiation at this intensity has little effect on the cell viability (Figures S11 and S12).

[32] a) M. Izquierdo-Serra, A. Bautista-Barrufet, A. Trapero, A. Garrido-Charles, A. Diaz-Tahoces, N. Camarero, S. Pittolo, S. Valbuena, A. Perez-Jimenez, M. Gay, A. Garcia-Moll, C. Rodriguez-Escrich, J. Lerma, P. de la Villa, E. Fernandez, M. A. Pericas, A. Llebaria, P. Gorostiza, *Nat. Commun.* **2016**, *7*, 12221; b) X. Fan, W. Y. Jin, J. Lu, J. Wang, Y. T. Wang, *Nat. Neurosci.* **2014**, *17*, 471–480.

[33] a) M. Gao, F. Yu, C. Lv, J. Choo, L. Chen, *Chem. Soc. Rev.* **2017**, *46*, 2237–2271; b) K. A. Ryu, C. M. Kaszuba, N. B. Bissonnette, R. C. Oslund, O. O. Fadeyi, *Nat. Chem. Rev.* **2021**, *5*, 322–337.

Manuscript received: November 14, 2021
Accepted manuscript online: February 23, 2022
Version of record online: March 4, 2022

© 2022 Wiley-VCH GmbH